Endometriosis: Contribution of 3.0-T Pelvic MR Imaging in Preoperative Assessment—Initial Results[1]

Nathalie Hottat, MD
Caroline Larrousse, MD
Vincent Anaf, MD, PhD
Jean-Christophe Noël, MD, PhD
Celso Matos, MD
Julie Absil, PhD
Thierry Metens, PhD

Purpose: To determine the accuracy of 3.0-T pelvic magnetic resonance (MR) imaging in the preoperative assessment of endometriosis and to evaluate colon wall involvement after intrarectal gel administration.

Materials and Methods: Institutional review board approval for this study was obtained, and each patient gave written informed consent. Forty-one consecutive patients with clinical suspicion of endometriosis underwent pelvic MR imaging at 3.0 T before surgery. Single-shot and high-spatial-resolution axial T2-weighted, sagittal fat-suppressed T2-weighted, and axial fat-suppressed T1-weighted sequences were performed. T2-weighted sequences were repeated after the rectum was filled with ultrasonographic (US) gel. Two blinded readers interpreted images independently. Image quality was scored by using a four-point scale. Detailed mapping of deep endometriosis was performed. Colon wall infiltration was graded (none, serosa, muscularis, submucosa, mucosa). MR imaging results were compared with surgical and pathologic findings. Interobserver agreement was assessed by using κ statistics. Nonparametric tests were performed to compare colon wall infiltration scores without and those with US gel and between observers.

Results: Twenty-seven of 41 patients had deep endometriosis at surgery and histopathologic examination. Sensitivity, specificity, positive and negative predictive values, and accuracy for the diagnosis of deep endometriosis at MR imaging were 96.3% (26 of 27), 100% (14 of 14), 100% (26 of 26), 93.3% (14 of 15), and 97.6% (40 of 41), respectively. κ Values ranged from 0.65 to 1.0, depending on the location of deep endometriosis. Colon wall infiltration assessment by both readers correlated well with pathologic findings (Spearman coefficient, >0.93), although median wall involvement scores were lower at pathologic examination than for both readers both before ($P = .042$ and $P = .011$) and after ($P = .079$ and $P = .011$) intrarectal gel filling.

Conclusion: MR imaging of the pelvis at 3.0 T is accurate in the diagnosis and staging of deep endometriosis for the preoperative assessment of patients clinically suspected of having endometriosis.

[1] From the Departments of Radiology (N.H., C.L., C.M., J.A., T.M.), Gynecology and Obstetrics (V.A.), and Pathology (J.C.N.), Erasme Hospital, Université Libre de Bruxelles, 808 Route de Lennik, B-1070 Brussels, Belgium. Received November 28, 2008; revision requested January 8, 2009; revision received March 11; accepted March 27; final version accepted April 27. **Address correspondence to** N.H. (e-mail: *nhottat@ulb.ac.be*).

Endometriosis is a benign chronic disease caused by the presence of ectopic endometrial glands and stroma outside the uterus. It is present in 10% of women at childbearing age and in 25%–35% of women with infertility (1). Endometriosis can cause crippling chronic pelvic pain, dysmenorrhea, dyspareunia, and infertility. Therefore, this disease can have a negative impact on everyday life and sexual life (2–7). Classically, endometriosis is classified into superficial and subperitoneal forms. Superficial endometriosis is related to the presence of hemorrhagic foci on the surface of the peritoneum and adhesions due to cyclic inflammation. Foci of endometriosis and adhesions are treated with laparoscopy (vaporization and adhesiolysis). Subperitoneal or deep endometriosis corresponds to an infiltration (>5 mm in depth) of the peritoneum and progressive extension into the Douglas pouch and beyond, with the endometriosis infiltrating the upper posterior part of the cervix, the uterosacral ligaments (USLs), the vagina, and/or the colon or, less often, the bladder and ureter (8,9). At pathologic examination, deep infiltrating endometriosis often takes the form of a nodular lesion consisting of smooth muscle and fibrosis with active glands and scanty stroma (10). Colon involvement represents a severe form and occurs with a frequency of 6%–30% of cases of deep endometriosis (8,11). The treatment of deep endometriosis consists of complete excision of the lesions.

Therefore, the diagnosis and staging of endometriosis should guide the surgeon to schedule the most appropriate one-step surgery: conservative laparoscopic treatment or open surgery with colonic resection if there is infiltrative parietal colon involvement (12–15). Magnetic resonance (MR) imaging at 1.5 T enables precise mapping of the lesions before surgery (16,17). In our study, we aimed to exploit the improved signal-to-noise ratio at 3.0 T to obtain images with a higher spatial resolution, which is desirable for the diagnosis and staging of deep endometriosis. The goal of this study was to determine the accuracy of 3.0-T pelvic MR imaging in the preoperative assessment of endometriosis and to evaluate colon wall involvement after intrarectal gel administration.

Advances in Knowledge

- MR imaging at 3.0 T yields high-spatial-resolution images that accurately depict all locations of deep endometriosis, including thin anatomic structures like the uterosacral ligaments and the colon wall.
- When compared with surgery and pathologic examination, 3.0-T MR imaging enables precise mapping of deep endometriosis, allowing an accurate diagnosis of deep endometriosis with a sensitivity of 96.3% (26 of 27) and a specificity of 100% (14 of 14).
- With high-spatial-resolution T2-weighted MR imaging sequences, the administration of intrarectal US gel did not improve the assessment of colon wall involvement.

Implication for Patient Care

- In patients with a clinical suspicion of endometriosis, a complete noninvasive preoperative assessment can be performed at 3.0-T MR imaging with excellent accuracy (97.6%) and without the administration of any contrast material.

Materials and Methods

Patients

Institutional review board approval was obtained, and patients gave written informed consent. Between March 2007 and August 2008, 106 consecutive patients referred for pelvic MR imaging because of a clinical suspicion of endometriosis were prospectively enrolled. Among these, 41 patients who underwent surgery were included in our study (mean age, 33 years; range, 20–46 years). Endometriosis was suspected because of one or more of the following symptoms: pelvic pain (29 of 41 patients), dysmenorrhea (19 of 41 patients), dyspareunia (five of 41 patients), suspicious results at clinical examination (15 of 41 patients), and recurrence of symptoms and a past history of endometriosis (seven of 41 patients). Exclusion criteria were the common contraindications to MR imaging (pacemaker, metallic foreign bodies, and claustrophobia), age younger than 18 years, and postmenopausal status.

MR Imaging

MR imaging was performed with patients in the supine position by using a 3.0-T MR imaging unit (Achieva; Philips Medical Systems, Best, the Netherlands) and a six-channel phased-array coil. The patients had been fasting for 6 hours before MR imaging. In order to reduce peristaltic movement artifacts, all patients received 20 mg of an antispasmodic drug (Buscopan [20 mg/1 mL]; Boehringer Ingelheim, Barcelona, Spain), that was slowly administered intravenously just before the beginning of the MR imaging examination. A rapid single-shot turbo spin-echo (TSE) T2-weighted sequence (18) was performed in the axial plane (repetition time msec/echo time msec, 4690/100; 32 sections; no section gap; spatial resolution, $0.7 \times 1.0 \times 4.0$ mm^3; field of view, 360×360 mm; echo train length, 73; sensitivity encoding acceleration factor, three; duration, 37.5 seconds), followed by a fat-suppressed TSE T2-weighted se-

Published online before print
10.1148/radiol.2531082113

Radiology 2009; 253:126–134

Abbreviations:
TSE = turbo spin echo
USL = uterosacral ligament

Author contributions:
Guarantors of integrity of entire study, N.H., C.M.; study concepts/study design or data acquisition or data analysis/interpretation, all authors; manuscript drafting or manuscript revision for important intellectual content, all authors; manuscript final version approval, all authors; literature research, N.H., V.A., J.A., T.M.; clinical studies, N.H., C.L., V.A., J.C.N.; experimental studies, V.A.; statistical analysis, V.A., J.A., T.M.; and manuscript editing, N.H., V.A., C.M., T.M.

Authors stated no financial relationship to disclose.

quence oriented in the axis of the uterus (3835/48; 30 sections; 0.3-mm section gap; spatial resolution, 0.66 × 0.83 × 3.0 mm^3; field of view, 200 × 200 mm; TSE factor, eight; fat suppression with spectral adiabatic inversion-recovery pulse with an inversion time of 80 msec, a repetition time of 225 msec, and a sensitivity encoding acceleration factor of two).

A high-spatial-resolution TSE T2-weighted flow-compensated sequence was then performed in the axial orientation by using respiratory triggering (echo time, 135 msec; 30 sections; 0.3-mm section gap; spatial resolution, 0.75 × 0.75 × 3.0 mm^3; field of view, 270 × 300 mm; TSE factor, 20; sensitivity encoding acceleration factor, two; typical duration, 5 minutes). A breath-hold three-dimensional fat-suppressed T1-weighted sequence was also performed in the axial orientation (3.3/1.65; flip angle, 10°; 100–140 sections; acquisition resolution, 1.55 × 1.55 × 3.0 mm; reconstruction thickness, 1.5 mm; field of view, 300 × 350 mm^2; turbo field-echo factor, 50–65; fat suppression with spectral adiabatic inversion-recovery pulse with an inversion time of 90 msec, a repetition time of 266 msec, and a sensitivity encoding acceleration factor of two; duration, 19 seconds). With the patient lying on her left side on the examination table and by using a plastic tube, the rectum was filled with 60–180 mL (according to individual tolerance) of ultrasonographic (US) gel at body temperature (Aquasonic 100; Parker Laboratories, Fairfield, NJ). Then, with the patient again lying in the supine position, another 20 mg of the antiperistaltic drug was slowly administered intravenously, and the same imaging sequences, except for the axial breath-hold three-dimensional fat-suppressed T1-weighted sequence, were repeated. MR imaging examinations were well tolerated by all but two patients, for whom the rectal filling was not performed because of anxiety.

Surgery and Pathologic Examination

Thirty-one patients underwent laparoscopy, three patients underwent laparoscopically assisted vaginal hysterectomy, and seven patients underwent laparotomy. The final diagnosis of endometriosis was given at surgery and at histopathologic examination: For each patient, the surgeon and the pathologist (V.A. and J.C.N., both with more than 10 years of experience in the evaluation of endometriosis) established a detailed report that included the location and number of lesions and the ex-

Table 1

Location of Deep Endometriosis Diagnosed at Surgery and Confirmed at Histopathologic Examination in 41 Patients

Location	No. of Patients
Pouch of Douglas	22 (54)
USL	21 (51)
Vagina	11 (27)
Colon wall	13 (32)
Small bowel	0
Vesicouterine pouch	12 (29)
Bladder	2 (5)
Ureter	0

Note.—Data in parentheses are percentages.

Figure 1

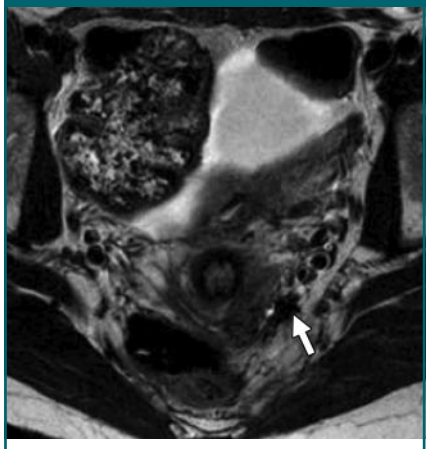

Figure 1: Axial high-spatial-resolution TSE T2-weighted flow-compensated MR image (repetition time, respiratory period; echo time, 135 msec) shows left USL involvement (arrow) in 24-year-old woman; this lesion was the false-negative instance of the diagnosis of deep endometriosis in our series and was seen retrospectively.

Table 2

Results of Reader Interpretation of MR Imaging Findings of Endometriosis Lesions in Different Locations

Lesion or Lesion Location	Reader 1 Sensitivity (%)	Reader 1 Specificity (%)	Reader 1 PPV (%)	Reader 1 NPV (%)	Reader 2 Sensitivity (%)	Reader 2 Specificity (%)	Reader 2 PPV (%)	Reader 2 NPV (%)	κ Value
Endometriomas*	96 (26/27)	98 (52/53)	96 (26/27)	98 (52/53)	93 (25/27)	98 (52/53)	96 (25/26)	96 (52/54)	0.97
Ovarian hemorrhagic foci†	67 (10/15)	92 (24/26)	83 (10/12)	83 (24/29)	67 (10/15)	81 (21/26)	67 (10/15)	81 (21/26)	0.84
Pouch of Douglas	95 (20/21)	100 (20/20)	100 (20/20)	95 (20/21)	95 (20/21)	100 (20/20)	100 (20/20)	95 (20/21)	1.0
USL*	80 (24/30)	96 (50/52)	92 (24/26)	89 (50/56)	90 (27/30)	79 (41/52)	70 (27/38)	93 (41/44)	0.65
Vesicouterine pouch	75 (6/8)	100 (33/33)	100 (6/6)	94 (33/35)	63 (5/8)	100 (33/33)	100 (5/5)	92 (33/36)	0.90
Bladder	50 (1/2)	100 (39/39)	100 (1/1)	98 (39/40)	50 (1/2)	100 (39/39)	100 (1/1)	98 (39/40)	1.0
Vagina	82 (9/11)	97 (29/30)	90 (9/10)	94 (29/31)	55 (6/11)	100 (30/30)	100 (6/6)	86 (30/35)	0.69
Colon wall without gel	100 (13/13)	96 (27/28)	93 (13/14)	100 (27/27)	100 (13/13)	96 (27/28)	93 (13/14)	100 (27/27)	0.89
Colon wall with gel	100 (13/13)	100 (26/26)	100 (13/13)	100 (26/26)	100 (13/13)	96 (25/26)	93 (13/14)	100 (25/25)	0.94

Note.—Numbers in parentheses are those used to calculate the percentages. NPV = negative predictive value, PPV = positive predictive value.

*Taking into account left and right locations separately.

†For ovaries, $n = 80$ because two patients had previously undergone unilateral oophorectomy.

tension of the lesions to pelvic organs, including the colon wall. Superficial peritoneal implants were treated with laser vaporization. Endometriomas and deep endometriosis lesions were excised and further analyzed at pathologic examination. Five patients had involvement of the colon serosa, and the surgeon performed meticulous dissection ("shaving") to preserve the colon wall. One patient had a frozen pelvis, with complete obliteration of the Douglas pouch, and underwent transrectal biopsies. Four patients underwent rectosigmoid nodule resection. Three patients underwent rectosigmoidectomy. The mean time between MR imaging and surgery was 60 days (range, 2–105 days). Surgical and histopathologic reports were used as the reference standard. When reports were conflicting, histopathologic results were used as the final reference standard. This affected the final diagnosis in one patient, in whom the surgical report described bilateral USL involvement but involvement of only one side was confirmed at histologic examination.

Image Analysis

Two investigators (N.H. [reader 1] and C.L. [reader 2], with 8 years and 1 year of experience in body MR imaging, respectively) who were blinded to clinical information independently and prospectively analyzed all MR images in two separate sessions by using viewing workstations (Viewforum; Philips Medical Systems). The two readers completed a standardized form. Image quality with T2-weighted sequences before and after rectal filling was graded on a scale from 0 to 3 (0 = noninterpretable, 1 = poor, 2 = satisfying, and 3 = excellent). The scale was based on the possibility of depicting such anatomic details as the ovarian parenchyma and follicles (<1 cm) and the colon and bladder walls. If image degradation occurred, readers were asked to look for an explanation. A systematic analysis of the pelvic cavity was performed, and the locations of the lesions were determined. The investigated locations were as follows: the uterus, the adnexa, the Douglas pouch, the USLs, the vagina, the small bowel, the colon wall (before and after rectal filling), the vesicouterine pouch, the bladder wall, and the ureters. The position of the uterus was described, and the thickness of the junctional zone was measured at three levels (anterior, posterior, and fundal). Adenomyosis was diagnosed when the junctional zone was 12 mm or greater (19).

The diagnosis of endometrioma was based on the identification of a cystic adnexal lesion with characteristics of chronic bleeding: hyperintensity on fat-suppressed T1-weighted images and a signal intensity decrease ("shading") on T2-weighted images (20,21). For each patient, we considered the right and left adnexa separately and stated whether or not endometrioma was present. Hemorrhagic ovarian lesions smaller than 1 cm were diagnosed as hemorrhagic foci and were counted. Results were summarized by reporting the presence or absence of hemorrhagic foci. Deep endometriosis was described as nodular or retractile fibrotic-like tissue that was hypointense on T2-weighted images and isointense to muscle on T1-weighted images (17,22). Adhesions and indirect signs of adhesions were also described. Adhesions were diagnosed as hypointense peritoneal strands that converged to loculated fluid collections or organ displacements. If colon involvement was suspected, the precise location (distance from the anorectal junction) was described and the length and depth of the lesion were measured with electronic calipers. Infiltration of the colon wall was described in different layers (none, serosa, muscularis, submucosa, mucosa) and was scored before and after rectal filling.

Figure 2

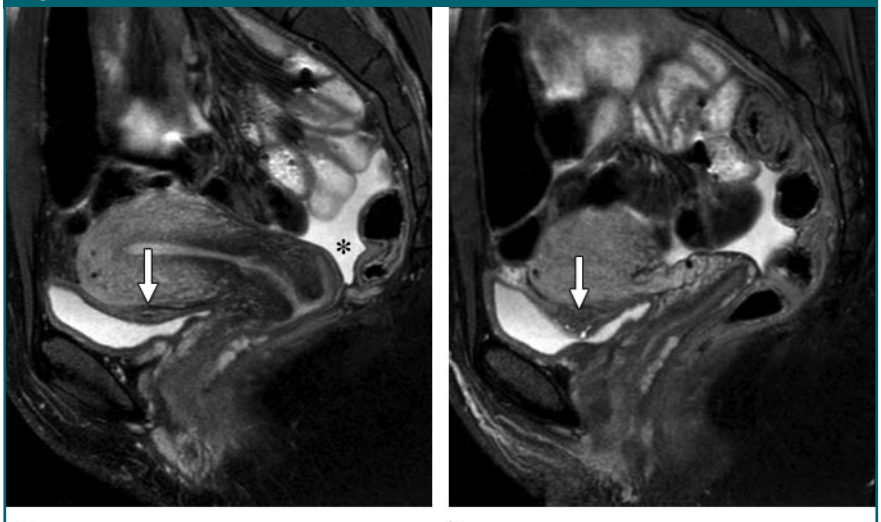

a. b.

Figure 2: **(a, b)** Sagittal fat-suppressed TSE T2-weighted MR images (3835/48) in 37-year-old woman show **(a)** normal appearance of the uterus, Douglas pouch (*), and vesicouterine pouch (arrow) and **(b)** deep endometriosis of the vesicouterine pouch infiltrating the bladder wall (arrow).

Statistical Analysis

A Wilcoxon paired test was used to compare the different sequences and the same sequences before and after administration of intrarectal US gel.

Sensitivity, specificity, and positive and negative predictive values were determined for the diagnosis of the different locations of endometriosis; for endometriomas and USL involvement, these calculations were made for left and right locations separately. To take into account the effect of repeated measurements in the same patient for endometriomas and USL involvement, sensitivity and specificity were recalculated on a per-patient basis. For the diagnosis of deep endometriosis, accuracy and the Youden index were added. Interobserver agreement was assessed with the Cohen κ coefficient; agreement was considered to be good when κ was be-

Figure 3

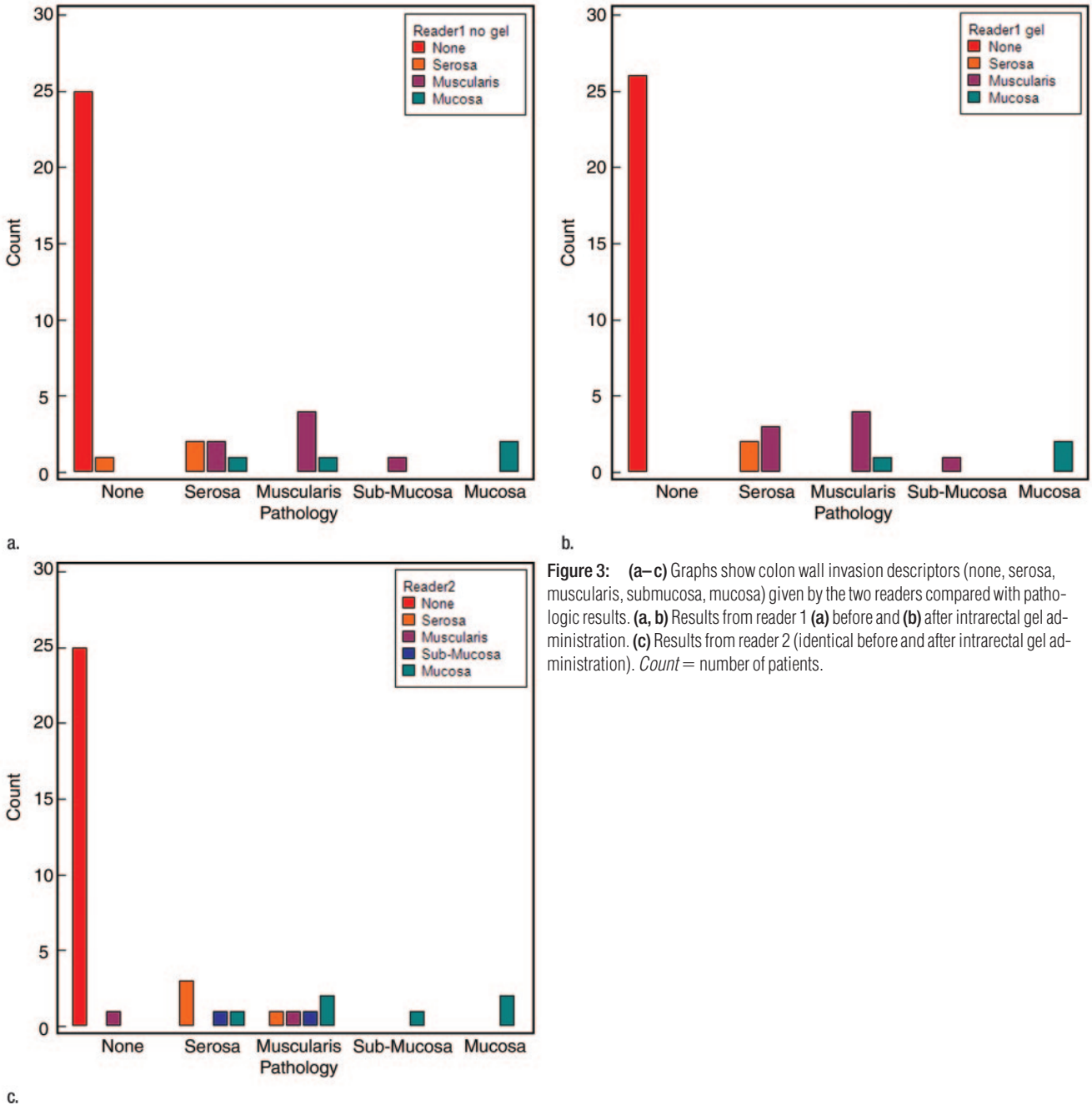

Figure 3: **(a–c)** Graphs show colon wall invasion descriptors (none, serosa, muscularis, submucosa, mucosa) given by the two readers compared with pathologic results. **(a, b)** Results from reader 1 **(a)** before and **(b)** after intrarectal gel administration. **(c)** Results from reader 2 (identical before and after intrarectal gel administration). *Count* = number of patients.

tween 0.6 and 0.8 and was considered to be excellent when κ was greater than 0.8. Nonparametric tests (Wilcoxon paired test, Spearman correlation coefficient) were performed to compare colon wall infiltration scores without and those with US gel and between observers. Linear weighted κ statistics were used to assess interobserver agreement in grading colon wall infiltration (23). The level of statistical significance was set at $P < .05$. For correlation coefficients, the P value and the power of the test were calculated.

Results

Image quality scores with the high-spatial-resolution TSE T2-weighted flow-compensated sequence were significantly higher than those with the rapid single-shot TSE T2-weighted sequence ($P <$

.001 without and with gel). Image quality with the rapid single-shot TSE T2-weighted sequence was improved after the administration of intrarectal US gel ($P = .039$), while administration of the gel degraded the image quality score with the fat-suppressed TSE T2-weighted sequence ($P < .001$) and the high-spatial-resolution TSE T2-weighted flow-compensated sequence ($P = .069$, not significant). Image degradation was due to bowel peristalsis.

In 27 (66%) of 41 patients, deep endometriosis was diagnosed at surgery and confirmed at histopathologic examination (Table 1). Three patients (7%) had endometrioma without deep endometriosis, and another three (7%) had adenomyosis only. These latter three patients underwent laparoscopically assisted vaginal hysterectomy, and adenomyosis was detected at MR imaging in all of them. MR imaging depicted adenomyosis in 10 of 41 patients, but standard-of-reference results were available for three patients only.

Four patients (10%) had superficial endometriosis only; two of these four patients had true-positive findings at MR imaging, where the diagnosis of superficial endometriosis was proposed because of adhesions and peritoneal irregularities. Another four patients (10%) had no endometriosis: One tubo-ovarian abscess and three normal sets of laparoscopic findings were correctly identified at MR imaging.

Regarding the 27 (66%) cases of deep endometriosis, at MR imaging there were 26 true-positive cases, one false-negative case in which the lesion was located on the left USL and the uterus was in an anteflexed position (Fig 1), no false-positive cases, and 14 true-negative cases. Sensitivity, specificity, positive predictive value, negative predictive value, and accuracy for the diagnosis of deep endometriosis by the two readers were identical and were 96.3% (26 of 27), 100% (14 of 14), 100% (26 of 26), 93.3% (14 of 15), and 97.6% (40 of 41), respectively (Youden index = 0.96). Overall, 16 patients had multiple locations of deep endometriosis. Detailed results for the different locations of deep endometriosis are given in Table 2.

The sensitivity and specificity, respectively, for endometriomas recalculated on a per-patient basis were 95% (20 of 21) and 95% (19 of 20) for reader 1 and 90% (19 of 21) and 95% (19 of 20) for reader 2. The sensitivity and specificity, respectively, for USL involvement recalculated on a per-patient basis were 82% (18 of 22) and 89% (17 of 19) for reader 1 and 91% (20 of 22) and 79% (15 of 19) for reader 2. The USLs were seen in 100% of the patients.

There were two cases of deep endometriosis with bladder involvement. Figure 2 illustrates a case of deep endometriosis located in the vesicouterine pouch with infiltration of the bladder wall. We missed one case in which the bladder was empty and the lesion was small (<1 cm) and confined to the serous layer of the bladder wall.

Figure 3 provides the colon wall infiltration scores at pathologic examination compared with the scores given by the two readers before and after intrarectal gel administration. Table 3 gives the Spearman correlation coefficient between both readers and pathologic examination for colon wall infiltration

Table 3

Spearman Correlation Coefficients for Colon Wall Infiltration Scores

Parameter	Reader 1 without Gel	Reader 2 without Gel	Reader 1 with Gel	Reader 2 with Gel	Pathologic Examination
Reader 1 without gel	1.0	0.903	0.970	0.900	0.954
Reader 2 without gel	. . .	1.0	0.930	1	0.940
Reader 1 with gel	. . .	. . .	1.0	0.930	0.987
Reader 2 with gel	. . .	. . .	. . .	1.0	0.937
Pathologic examination	. . .	. . .	. . .	. . .	1.0

Note.—The Spearman coefficient was significant at the level of $P = .01$, with a test power that was larger than 0.95; 41 patients were examined without intrarectal US gel and 39 patients were examined with intrarectal US gel.

Figure 4

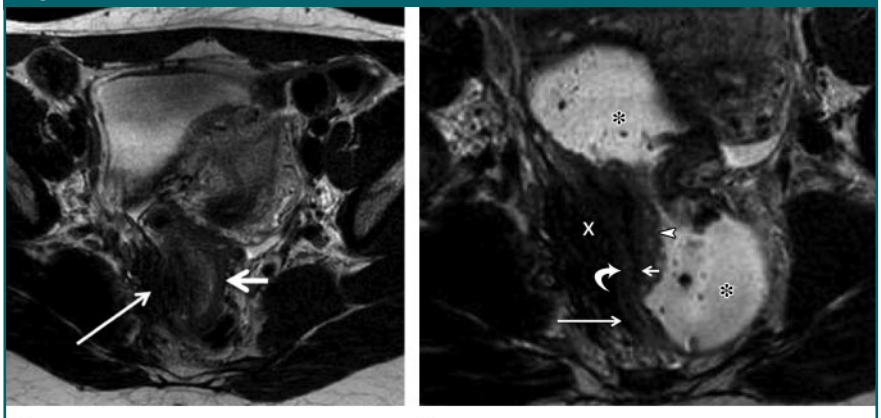

Figure 4: **(a, b)** Axial high-spatial-resolution TSE T2-weighted flow-compensated T2-weighted MR images (repetition time, respiratory period; echo time, 135 msec) in 21-year-old woman. **(a)** There is deep endometriosis infiltrating the right USL (short arrow), pelvic muscle, and colon wall (long arrow). **(b)** Image shows circumferential rectosigmoid stenosis due to deep endometriosis *(x)* visualized after administration of intrarectal US gel (* = rectosigmoid lumen filled with gel). The different sublayers can be distinguished (arrowhead = mucosa, short straight arrow = submucosa, curved arrow = muscularis, long straight arrow = serosa). At MR imaging and pathologic examination, the colon wall infiltration was graded as involving the mucosa.

Figure 5

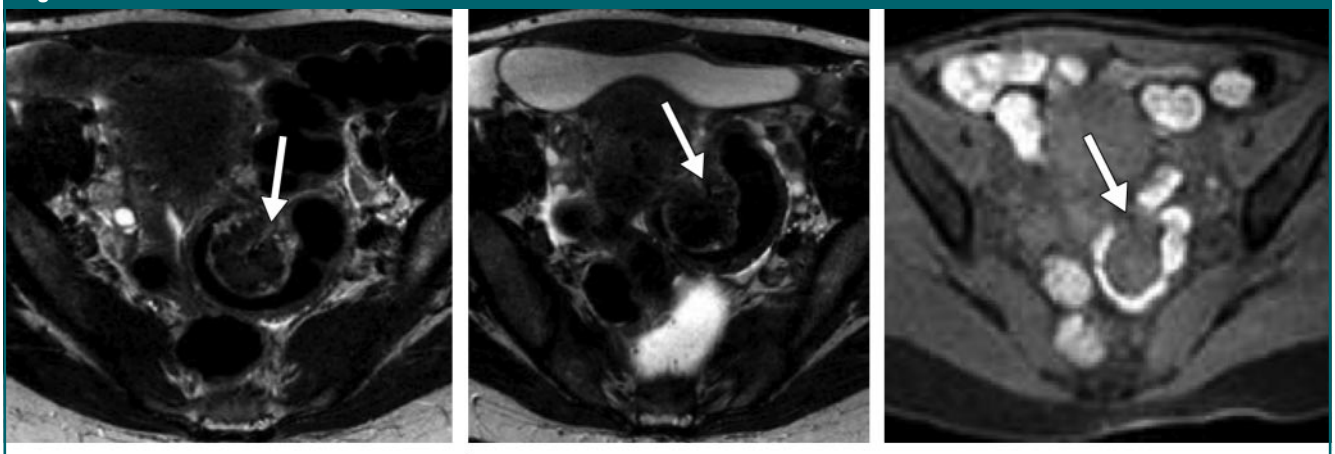

a. b. c.

Figure 5: **(a)** Axial T2-weighted MR image (repetition time, respiratory period; echo time, 135 msec) obtained before rectal filling with US gel in 32-year-old woman shows deep endometriosis involving the sigmoid colon with a bulging lesion (arrow). At both MR imaging and pathologic examination, the colon wall infiltration was graded as involving the muscularis layer. **(b)** Axial T2-weighted MR image (repetition time, respiratory period; echo time, 135 msec) obtained after rectal filling with US gel. The gel is visible in the rectum but did not reach the sigmoid level. The same lesion (arrow) is seen. **(c)** On axial breath-hold three-dimensional fat-suppressed T1-weighted MR image (3.3/1.65; flip angle, 10°), the rectosigmoid contents appear hyperintense (arrow) and provide good depiction of the lesion boundaries without administration of intrarectal US gel.

scores, and this coefficient was greater than 0.93 when the readers' results were compared with pathologic examination results. The differences in colon wall infiltration scores between reader 1 and reader 2 were not significant before or after administration of intrarectal US gel ($P = .296$ before and $P = .102$ after administration of gel, bilateral Wilcoxon test). The linear weighted Cohen κ coefficients were 0.72 and 0.73, respectively, for the infiltration scores before and after administration of intrarectal gel (Fig 4). For reader 1, the scores before and after administration of intrarectal gel were not significantly different ($P = .18$). The scores for reader 2 were identical before and after administration of intrarectal gel (Fig 5). The colon wall infiltration scores at pathologic examination were lower than those of both readers before ($P = .042$ for reader 1 and $P = .011$ for reader 2, unilateral Wilcoxon test) and after ($P = .079$ for reader 1 and $P = .011$ for reader 2) administration of intrarectal gel.

Discussion

Our study results show an excellent correlation of MR imaging findings with surgical and histopathologic examination findings of adnexal and deep endometriosis. Both readers detected endometriomas with a high sensitivity (>93%) and specificity (98%).

The main objective of our study was to assess the presence of deep endometriosis lesions and to depict their specific locations. Operating at 3.0 T, we obtained sensitivity, specificity, positive predictive, negative predictive, and accuracy values, respectively, of 96.3%, 100%, 100%, 93.3%, and 97.6% for diagnosing deep endometriosis. In comparison, Bazot et al (16) reported sensitivity, specificity, positive predictive, negative predictive, and accuracy values of 90.3%, 91%, 92.1%, 89%, and 90.8%, respectively, for the diagnosis of deep endometriosis in a large series at 1.5 T. The excellent negative predictive value, 93.3% (14 of 15), for the diagnosis of deep endometriosis achieved in our study could influence the surgeon to perform laparoscopy of superficial endometriosis rather than more extensive surgery.

However, precise preoperative mapping of deep endometrial lesions is useful for guiding the surgeon, especially in forms of endometriosis with substantial adhesions and an obliterated Douglas pouch that can hide lesions involving the rectosigmoid colon.

The image quality with our respiratory-triggered high-spatial-resolution TSE T2-weighted flow-compensated sequence was significantly better than that with rapid single-shot TSE T2-weighted sequences after antiperistaltic drug injection without intrarectal contrast material. After rectal filling with US gel, the image quality with the fat-suppressed TSE T2-weighted sequence was significantly degraded because of bowel peristalsis, despite another injection of the antiperistaltic drug, while the image quality with the high-spatial-resolution TSE T2-weighted flow-compensated sequence remained better than that with the rapid single-shot TSE T2-weighted sequence.

In our study, as well as in the literature, the USLs and the Douglas pouch are the most common locations of deep endometriosis; the prevalence of USL involvement was 51% in our study and ranges between 46% and 69% in the literature, depending on the series (8,9,16,22,24). In our study, the USLs (normal or abnormal) were seen in 100% of the patients. The less experienced reader reported 11 false-positive instances of USL in-

volvement. This could be explained by the difficulty of distinguishing surgical sequelae from recurrences of deep endometriosis, explaining the lowest interobserver agreement value obtained in our study ($\kappa = 0.65$). In most of the other endometriosis locations, the agreement between readers was excellent ($\kappa > 0.8$). In the false-negative case of the diagnosis of deep endometriosis, the lesion was located on the left USL. Classically, the causes of misinterpretation of USL involvement are a retroflexed uterus or the interposition of endometriomas or bowel loops (16). However, in our case, the uterus was in an anteflexed position, and the lesion was seen retrospectively.

In our series, the prevalence of colon wall involvement was high (32%) compared with the prevalence reported in the literature (8,11). This could be explained by recruitment bias, as our institution is a tertiary referral center for colon surgery. At 3.0 T and with T2-weighted high-spatial-resolution sequences, it was possible to distinguish the different layers of the involved colon without gadolinium-enhanced T1-weighted imaging. Our study showed an excellent correlation (with Spearman coefficients > 0.93) between MR imaging and histopathologic examination for the degree of invasion of the colon wall. However, in some patients with colon wall involvement, both readers gave colon wall invasion scores that were higher than the scores at pathologic examination.

Intrarectal US gel was administrated to improve the contrast between the rectal lumen and the wall. The administration of this gel was well tolerated in the majority of our patients. In our study, US gel distended the rectum and could generate movement artifacts that might degrade image quality. Another disadvantage appeared when the US gel did not go far enough upward: Multifocal or upper lesions (eg, sigmoid and cecal lesions) could be missed because of the lack of contrast. Overall, in our study no significant advantage was found after rectal filling, with no additional lesion diagnosed; only one false-positive case of colon wall invasion was reassigned as negative (by reader 1) after gel administration.

Anterior deep endometriosis is much less frequent than posterior involvement and involves the vesicouterine pouch and the bladder. Bladder involvement occurs in 2%–6.4% of patients, depending on the series (25–27), and MR imaging performs better than cystoscopy in the diagnosis of anterior endometriosis. In our study, we had two cases of anterior deep endometriosis that infiltrated the bladder; one case was correctly identified and we missed the other case, but the bladder was empty and the lesion was small (<1 cm) and confined to the serous layer of the bladder wall. Interestingly, the agreement between the two readers was almost perfect in the assessment of the vesicouterine pouch and the bladder ($\kappa = 0.90$ and $\kappa = 1.0$, respectively).

Laparoscopy is the reference standard for the diagnosis of superficial endometriosis, and the peritoneal implants of endometriosis are difficult to diagnose with MR imaging (22,25). In our study, superficial endometriosis not associated with deep lesions was correctly identified in two of four cases.

The assessment of endometriosis may be laborious for the patient, who may undergo multiple examinations like transvaginal US, transrectal US, barium enema, cystoscopy, and rectoscopy. Instead, MR imaging at 3.0 T enables complete exploration of the pelvis (peritoneal and subperitoneal spaces) with a relatively high spatial resolution and therefore could be the preoperative imaging technique of choice for the assessment of patients with a clinical suspicion of deep endometriosis. Indeed, in our series, T2-weighted high-spatial-resolution images acquired at 3.0 T allowed the detection of thin structures such as the USLs and the colon and bladder walls.

In addition to recruitment bias, our study had other limitations. The patient sample size ($n = 41$) seems reasonable, but further experience is necessary to confirm our data, especially for colon involvement (13 patients). Another limitation was the mean time of 60 days between the MR imaging examination and the surgery; however, because deep endometriosis is a chronic disease, we expect that this delay would not dramatically bias our results. Not all 106 patients underwent surgery, so we do not know the accuracy of 3.0-T MR imaging in our total study population. Including only patients who underwent surgery likely skewed our results. Our surgeon knew the results of the MR imaging examination, and this could have biased results at surgery. Finally, because our population was selected in a referral center, it was biased for the prevalence of endometriosis.

In conclusion, pelvic MR imaging at 3.0 T provides encouraging results for the diagnosis and the preoperative staging of deep endometriosis, especially for USL and colon wall involvement, with excellent interobserver agreement.

Acknowledgments: We thank Viviane De Maertelaer, PhD, Department of Medical Statistics, Université Libre de Bruxelles, Brussels, Belgium and Frédéric Buxant, MD, Dario Bucella, MD, Jean-Frédéric Limbosch, MD, and Philippe Simon, MD, PhD, Department of Gynecology and Obstetrics, Erasme Hospital, Université Libre de Bruxelles, Brussels, Belgium.

References

1. Viganò P, Parazzini F, Somigliana E, Vercellini P. Endometriosis: epidemiology and aetiological factors. Best Pract Res Clin Obstet Gynaecol 2004;18(2):177–200.
2. Cornillie FJ, Oosterlynck D, Lauweryns JM, Koninckx PR. Deeply infiltrating pelvic endometriosis: histology and clinical significance. Fertil Steril 1990;53(6):978–983.
3. Koninckx PR, Meuleman C, Demeyere S, Lesaffre E, Cornillie FJ. Suggestive evidence that pelvic endometriosis is a progressive disease, whereas deeply infiltrating endometriosis is associated with pelvic pain. Fertil Steril 1991;55(4):759–765.
4. Anaf V, Simon P, El Nakadi I, et al. Relationship between endometriotic foci and nerves in rectovaginal endometriotic nodules. Hum Reprod 2000;15(8):1744–1750.
5. Anaf V, Simon P, El Nakadi I, et al. Hyperalgesia, nerve infiltration and nerve growth factor expression in deep adenomyotic nodules. Hum Reprod 2002;17(7):1895–1900.
6. Anaf V, Chapron C, El Nakadi I, De Moor V, Simonart T, Noël JC. Pain, mast cells and

nerves in peritoneal, ovarian and deep infiltrating endometriosis. Fertil Steril 2006; 86(5):1336–1343.

7. Anaf V, Simon P, El Nakadi I, Simonart T, Noel J, Buxant F. Impact of surgical resection of rectovaginal pouch of Douglas endometriotic nodules on pelvic pain and some elements of patient's sex life. J Am Assoc Gynecol Laparosc 2001;8(1):55–60.
8. Chapron C, Fauconnier A, Vieira M, et al. Anatomical distribution of deeply infiltrating endometriosis: surgical implications and proposition for a classification. Hum Reprod 2003;18(1):157–161.
9. Chapron C, Chopin N, Borghese B, et al. Deeply infiltrating endometriosis: pathogenetic implications of the anatomical distribution. Hum Reprod 2006;21(7):1839–1845.
10. Anaf V, Simon P, Fayt I, Noel J. Smooth muscles are frequent components of endometriotic lesions. Hum Reprod 2000;15(4): 767–771.
11. Nisolle M, Donnez J. Peritoneal endometriosis, ovarian endometriosis and adenomyotic nodules of the rectovaginal septum are three different entities. Fertil Steril 1997;68(4): 585–596.
12. Régenet N, Métairie S, Cousin GM, Lehur PA. Colorectal endometriosis: diagnosis and management [in French]. Ann Chir 2001; 126(8):734–742.
13. Abbott JA, Hawe J, Clayton RD, Garry R. The effects and effectiveness of laparoscopic excision of endometriosis: a prospective study with 2–5 year follow-up. Hum Reprod 2003;18(9):1922–1927.
14. Wykes CB, Clark TJ, Chakravati S, Mann CH, Gupta JK. Efficacy of laparoscopic excision of visually diagnosed peritoneal endometriosis in the treatment of chronic pelvic pain. Eur J Obstet Gynecol Reprod Biol 2006;125(1):129–133.
15. Chopin N, Vieira M, Borghese B, et al. Operative management of deeply infiltrating endometriosis: results on pelvic pain symptoms according to surgical classification. J Minim Invasive Gynecol 2005;12(2):106–112.
16. Bazot M, Darai E, Hourani R, et al. Deep pelvic endometriosis: MR imaging for diagnosis and prediction of extension of disease. Radiology 2004;232(2):379–389.
17. Kinkel K, Frei KA, Balleyguier C, Chapron C. Diagnosis of endometriosis with imaging: a review. Eur Radiol 2006;16(2):285–2987.
18. Morakkabati-Spitz N, Schild HH, Kuhl CK, et al. Female pelvis: MR imaging at 3.0 T with sensitivity encoding and flip-angle sweep technique. Radiology 2006;241(2): 538–545.
19. Reinhold C, McCarthy S, Bret PM, et al. Diffuse adenomyosis: comparison of endovaginal US and MR imaging with histopathologic correlation. Radiology 1996;199(1): 151–158.
20. Togashi K, Nishimura K, Kimura I, et al. Endometrial cysts: diagnosis with MR imaging. Radiology 1991;180(1):73–78.
21. Woodward PJ, Sohaey R, Mezzetti TP Jr. Endometriosis: radiologic-pathologic correlation. RadioGraphics 2001;21(1):193–216.
22. Kinkel K, Chapron C, Balleyguier C, Fritel X, Dubuisson JB, Moreau JF. Magnetic resonance imaging characteristics of deep endometriosis. Hum Reprod 1999;14(4):1080–1086.
23. Kundel HL, Polansky M. Measurement of observer agreement. Radiology 2003; 228(2):303–308.
24. Chapron C, Dubuisson JB, Tardif D, Decoret E. Retroperitoneal endometriosis infiltrating the utero-sacral ligaments: technique and results of laparoscopic surgery [in French]. J Gynecol Obstet Biol Reprod (Paris) 1997; 26(3):264–269.
25. Del Frate C, Girometti R, Pittino M, Del Frate G, Bazzocchi M, Zuiani C. Deep retroperitoneal pelvic endometriosis: MR imaging appearance with laparoscopic correlation. RadioGraphics 2006;26(6):1705–1718.
26. Vercellini P, Meschia M, De Giorgi O, Panazza S, Cortesi I, Crosignani PG. Bladder detrusor endometriosis: clinical and pathogenic implications. J Urol 1996; 155(1):84–86.
27. Balleyguier C, Chapron C, Dubuisson JB, et al. Comparison of magnetic resonance imaging and transvaginal ultrasonography in diagnosing bladder endometriosis. J Am Assoc Gynecol Laparosc 2002;9(1):15–23.